

phys. stat. sol. (b) **109**, 83 (1982)

Subject classification: 13.4 and 19; 22.1.2

Natuurkundig Laboratorium der Universiteit van Amsterdam¹⁾ (a) and Institute for the Study of Defects in Solids, Department of Physics, State University of New York at Albany²⁾ (b)

EPR Observation of an Au-Fe Complex in Silicon

II. Electronic Structure³⁾

By

E. G. SIEVERTS (a), S. H. MULLER (a), C. A. J. AMMERLAAN (a),
R. L. KLEINHENZ (b), and J. W. CORBETT (b)

For a description of the Au-Fe complex which is discussed in Part I of this article, a model by Ludwig and Woodbury is adopted. This model does not allow for an analysis of the observed hyperfine interactions in a simple LCAO description. Instead a model of exchange coupled spins is proposed. The calculated actual hyperfine interactions are compared with data of atomic wave functions for Au and Fe. Due to covalency and/or hybridization effects the quantities $\langle r^{-3} \rangle_d$ which characterize the d-orbitals on the Fe and Au atoms are considerably reduced in silicon with respect to the free atoms. As a result, the s-core polarization effects which determine the isotropic hyperfine interactions are found to be weaker in a silicon matrix than in most other materials.

Mit Hilfe eines Modells von Ludwig und Woodbury wird der Au-Fe-Komplex beschrieben, der in Teil I dieser Arbeit eingeführt wurde. Dieses Modell ist allerdings nicht für die Analyse der beobachteten Hyperfeinwechselwirkungen mittels Linearkombinationen atomarer Wellenfunktionen geeignet. Daher wird ein Modell austauschgekoppelter Elektronenspins vorgeschlagen. Damit werden die wirklichen Hyperfeinwechselwirkungen berechnet und mit atomaren Wellenfunktionsdaten von Gold und Eisen verglichen. Kovalenz- oder Hybrid-Effekte reduzieren die $\langle r^{-3} \rangle_d$ -Werte, die die d-Orbitale der Gold- und Eisen-Atome im Silizium charakterisieren, im Vergleich zu denen der freien Atome. Die Polarisations-Effekte der inneren s-Elektronen-Schale, die für den isotropen Teil der Hyperfeinwechselwirkung verantwortlich sind, sind daher in der Silizium-Matrix auch beträchtlich schwächer als in den meisten anderen Materialien.

1. Introduction

In the early 1960's Ludwig and Woodbury proposed a highly successful model for the description of transition metal impurities in silicon [1 to 3]. With the use of EPR they extensively studied a series of substitutional and interstitial 3d transition metal impurities in various charge states. In the framework of their model they were able to account for the observed electron spin in all cases. If the effective orbital momentum was not equal zero, they were able to calculate the observed deviations of the spectroscopic splitting factor from $g \approx 2$, with the use of an adapted Landé formula. Also Jahn-Teller effects could be explained or predicted. Since their work relatively little effort has been spent in this field. Only recently there is renewed interest in transition metal impurities in silicon (see [15 to 21] of Part I).

In view of the success of the original work by Ludwig and Woodbury, it is appropriate to adopt their theory for the basic description of the present problem. They

¹⁾ Valckenierstraat 65, 1018 XE Amsterdam, The Netherlands.

²⁾ Albany, NY 12222, USA.

³⁾ Part I see phys. stat. sol. (b) **108**, 363 (1981).

distinguish the cases of substitutional and interstitial impurities in the silicon lattice. A substitutional atom is required to establish covalent tetrahedral bonds with its four nearest neighbours. This will be achieved by promotion of d-electrons and subsequent sp^3 hybridization, in order to arrive at a $3d^n4s4p^3$ configuration. Due to the crystal field of the silicon lattice, the energy levels of the d-electrons will split into a t_2 triplet and an e doublet, overlap with nearby lattice sites causing the triplet state with the d_{xy} , d_{yz} , and d_{zx} orbitals to have a higher energy than the doublet state with the $d_{x^2-y^2}$ and d_{z^2} orbitals. According to Ludwig and Woodbury a weak crystal field approximation holds in a covalent solid such as silicon, so that Hund's rule has to be applied when filling the five 3d levels with the remaining n electrons.

An interstitial transition metal impurity, they argued, needs no covalent bonding. In the silicon environment all electrons will be confined to the 3d shell, resulting in a pure $3d^n$ configuration. For the tetrahedral interstitial position, the order of triplet and doublet d-electron levels is reversed, the doublet having higher energy. Again Hund's rule applies.

The most common interstitial transition metal impurity in silicon is iron. If neutral it gives rise to a $3d^8$ configuration. Due to two missing electrons in the 3d doublet level, an orbital singlet state with an electronic spin value $S = 1$ and an effective angular momentum value $L' = 0$ results. The isotropic resonance of iron at $g = 2.070$ is one of the most extensively studied spectra in silicon [1 to 5]. The $3d^7$ configuration of Fe_i^+ does not have an orbital singlet ground state as one electron is missing from the 3d triplet level. The resulting dynamic Jahn-Teller distortion yields an isotropic resonance. This state with $S = 3/2$ and $L' = 1$ gives $J = 1/2$ and $g \approx 10/3$ (actually $g = 3.52$) [1, 3].

For 4d and 5d transition elements essentially the same model is expected to apply. In this case the observed spectra for Pd_i^- and Pt_i^- require a bound hole, additional to the d^8-sp^3 configuration [6]. Gold is generally assumed to occupy substitutional positions in silicon. A $5d^76s6p^3$ configuration for Au_s^0 would result in an orbital singlet state with $S = 3/2$ and $L' = 0$. As discussed in the previous paper I, no EPR spectrum from isolated gold atoms has ever been observed. Only paired with other impurities, like Cr or Mn [3, 7] or Fe, has gold been recognized in EPR. Nevertheless it is one of the most extensively studied impurities in silicon [8]. On the basis of theoretical calculations, van Vechten and Thurmond [9] suggest an [interstitial Au + + vacancy] complex to describe gold in silicon. In view of its versatility we will further adopt the original model by Ludwig and Woodbury.

In this work we will try to give an analysis of the observed hyperfine interactions of the Au-Fe pair as described in Part I. Such an analysis is generally carried out on a particular choice of wave function for the unpaired electron. For deep level imperfections in silicon, linear combinations of atomic wave functions have often proved appropriate [10]. The position of an energy level far from either of the band edges and the consequent localization of the electron primarily upon few lattice sites, favours an LCAO description above one with Bloch-like lattice states. Especially for radiation defects in silicon and their complexes with impurities, this approach has been very successful. In the following we will show that it cannot be applied without adaptation to transition metal complexes. A brief discussion of the LCAO approach will be given in the next section, as well as a description of the effect of coupling of two localized electron spins as follow from the Ludwig-Woodbury picture.

Data on atomic wave functions for gold and iron as required for an analysis of the hyperfine interactions are collected in Section 3. The experimental data are compared with those collected in Section 3, in order to arrive at a detailed electronic model of the Au-Fe complex.

2. Theoretical Treatment

2.1 Hyperfine and quadrupolar interaction in the LCAO description

For many defects in silicon a one-electron description is sufficient to account for the phenomena observed with EPR. The wave function of the unpaired resonance electron is generally described as a linear combination of atomic orbitals which are centered on a few atoms around the paramagnetic center. In the case of radiation defects they generally comprise just s- and p-orbitals. For transition metal impurities, atomic d-orbitals should also be included. Summing over atomic sites i , a wave function has the form

$$\Psi = \sum_i \eta_i (\alpha_i \psi_s^i + \beta_i \psi_p^i + \gamma_i \psi_d^i). \quad (1)$$

For the sites of ^{29}Si nuclei ($I = 1/2$, 4.7% abundant) one takes $\gamma_i = 0$, while α_i and β_i refer to the atomic 3s and 3p orbitals. For transition metals, primarily d-orbitals are important, while s- and p-orbitals may be mixed in.

The wave function (1) gives rise to a hyperfine interaction with nucleus i of the form $\mathbf{A}_i = a_i \mathbf{1} + \mathbf{B}_i$. The isotropic part, which is the Fermi contact interaction, equals

$$a_i = \frac{8}{3} \pi g \mu_B g_N \mu_N \eta_i^2 \alpha_i^2 |\psi_s^i(0)|^2. \quad (2)$$

Here $|\psi_s^i(0)|^2$ is the electron density of the relevant atomic ns orbital of atom i at the site of its nucleus.

For either an atomic p- or d-orbital, the anisotropic part \mathbf{B}_i is axially symmetric with $B_{\parallel}^i = -2B_{\perp}^i = 2b_i$ and

$$b_i = \frac{2}{5} g \mu_B g_N \mu_N \eta_i^2 \beta_i^2 \langle r^{-3} \rangle_p^i \quad \text{or} \quad \frac{2}{7} g \mu_B g_N \mu_N \eta_i^2 \gamma_i^2 \langle r^{-3} \rangle_d^i. \quad (3)$$

Here $\langle r^{-3} \rangle$ is the expectation value of r^{-3} , weighted over the atomic p- or d-orbital. Information about the wave function as contained in the parameters η_i^2 , α_i^2 , β_i^2 , and γ_i^2 can be obtained if the atomic wave function parameters $|\psi_s^i(0)|^2$ and $\langle r^{-3} \rangle_{p/d}$ are known. For a number of elements, values have been estimated from both theoretical and experimental data (e.g. [10]). Data for Au and Fe will be given in the next section.

The electron wave function is also reflected in the nuclear quadrupole interaction through the interaction of the electric quadrupole moment of a nucleus with the electric field gradient from the surrounding electron distribution. The interaction parameter as determined by EPR can be written:

$$P = \frac{eQ}{4I(2I-1)} \frac{\partial^2 V}{\partial z^2} \quad (4)$$

in which Q is the nuclear electric quadrupole moment and $\partial^2 V / \partial z^2$ is the electric field gradient in the axial z -direction (see e.g. [11]). The field gradient is completely determined by the wave function configuration.

An enumeration of the effects of different atomic orbitals has been given by Townes and Dailey [12]. Closed shells and electrons in s-orbitals do not contribute to a field gradient. In general, the lowest incompletely filled p-orbital determines the field gradient mostly. For transition metal ions, d-orbitals are prominent in determining their physical properties, so that one should always carefully consider which orbitals to include. Also in the formula for the field gradient the expectation value of r^{-3} enters:

$$\frac{\partial^2 V}{\partial z^2} = \frac{4}{5} e \langle r^{-3} \rangle_p \quad \text{[or} \quad \frac{4}{7} e \langle r^{-3} \rangle_d. \quad (5)$$

Substitution of the LCAO wave function (1) results in

$$P = \frac{e^2 Q}{I(2I-1)} \frac{1}{5} \eta_i^2 \beta_i^2 \langle r^{-3} \rangle_p \quad \text{or} \quad \frac{e^2 Q}{I(2I-1)} \frac{1}{7} \eta_i^2 \gamma_i^2 \langle r^{-3} \rangle_d. \quad (6)$$

The electronic structure of transition metal impurities in silicon imposes serious restrictions on an LCAO treatment. There are a number of electrons or holes in the d-shell, whose electron spins sum up according to Hund's rule, so that a one-electron description is not appropriate. Fractions of electrons should no longer appear in (3) and (6), but instead the *total* unpaired electron spin density and the *total* electron charge density should enter. This can give rise to two different expectation values $\langle r^{-3} \rangle$ for a particular d-shell configuration. As long as Hund's rule applies the two values will be the same.

2.2 Exchange coupled spins

A serious problem for the use of an LCAO wave function results from the fact that the present EPR spectrum arises from a complex of two transition metal impurities. Each of them has its own d-shell configuration, each giving a total electron spin according to Hund's rule. In Part I we found that the paramagnetic Au-Fe center can effectively be described with a spin Hamiltonian with a single spin $S = 1/2$. In the Ludwig-Woodbury description Au_s^0 and Fe_i^0 give rise to effective electron spins $S_1 = 3/2$ and $S_2 = 1$, respectively. These spins can give rise to a total spin with values $S = 1/2$, $3/2$, or $5/2$. The same values result when $S_1 = 1$ and $S_2 = 3/2$, as is the case for $\text{Au}_s^- \text{Fe}_i^+$ which in Part I is considered the more probable state. In order to arrive at the observed effective spin, the $S = 1/2$ state has to be the ground state of the system of two exchange coupled spins. This will be the case if there is an antiferromagnetic interaction.

At this stage it is important to find how the hyperfine interactions of the individual spins S_1 and S_2 with the individual nuclear spins I_1 and I_2 translate into the interactions with the effective total spin in the spin Hamiltonian in Part I. The fact that this spin Hamiltonian with effective spin $S = 1/2$ gives an accurate description of the

Table 1

Base functions of a total spin S' as expressed in the original base functions of the constituent spins $S_1 = 3/2$ and $S_2 = 1$. Energy eigenvalues of the exchange interaction and relations between hyperfine interaction parameters are given

S'	$m_{S'}$	base functions of S_1 and S_2	energy	hyperfine interaction parameters	
				A'_1	A'_2
$\frac{5}{2}$	$\pm \frac{5}{2}$	$ \pm \frac{3}{2}, \pm 1\rangle$	$\frac{3}{2} J$	$\frac{3}{5} A_1$	$\frac{2}{5} A_2$
	$\pm \frac{3}{2}$	$\frac{1}{5} \sqrt{10} \pm \frac{3}{2}, 0\rangle + \frac{1}{5} \sqrt{15} \pm \frac{1}{2}, \pm 1\rangle$			
	$\pm \frac{1}{2}$	$\frac{1}{10} \sqrt{10} \pm \frac{3}{2}, \mp 1\rangle + \frac{1}{5} \sqrt{15} \pm \frac{1}{2}, 0\rangle + \frac{1}{10} \sqrt{30} \mp \frac{1}{2}, \pm 1\rangle$			
$\frac{3}{2}$	$\pm \frac{3}{2}$	$\frac{1}{5} \sqrt{15} \pm \frac{3}{2}, 0\rangle - \frac{1}{5} \sqrt{10} \pm \frac{1}{2}, \pm 1\rangle$	$-J$	$\frac{11}{15} A_1$	$\frac{4}{15} A_2$
	$\pm \frac{1}{2}$	$\frac{1}{5} \sqrt{10} \pm \frac{3}{2}, \mp 1\rangle + \frac{1}{15} \sqrt{15} \pm \frac{1}{2}, 0\rangle - \frac{2}{15} \sqrt{30} \mp \frac{1}{2}, \pm 1\rangle$			
$\frac{1}{2}$	$\pm \frac{1}{2}$	$\frac{1}{2} \sqrt{2} \pm \frac{3}{2}, \mp 1\rangle - \frac{1}{3} \sqrt{3} \pm \frac{1}{2}, 0\rangle + \frac{1}{6} \sqrt{6} \mp \frac{1}{2}, \pm 1\rangle$	$-\frac{5}{2} J$	$\frac{5}{3} A_1$	$-\frac{2}{3} A_2$

system, indicates that an exchange interaction term has to be large with respect to the Zeeman interaction. For transition metal ions, large exchange interactions tend to be very common. In this case an unperturbed spin Hamiltonian $\mathcal{H} = J\mathbf{S}_1 \cdot \mathbf{S}_2$ is allowed to operate upon the twelve base functions $|m_{S_1}, m_{S_2}\rangle$ which are the eigenfunctions of the operators S_{1z} , S_{2z} , S_1^2 , and S_2^2 . The resulting matrix can be diagonalized by taking combinations as given in Table 1. In this way the Hamiltonian matrix reduces to three blocks of dimensions six, four, and two, which can equivalently be described by effective spins \mathbf{S}' with values of 5/2, 3/2, and 1/2 and corresponding spin quantum numbers $m_{S'}$. In the case of antiferromagnetic exchange ($J > 0$), $S' = 1/2$ is the ground state, the next state being $(3/2)J$ higher in energy.

The most important term to add as a perturbation is the hyperfine interaction. For simplicity we restrict ourselves to an isotropic interaction

$$\mathcal{H}^{(1)} = A_1\mathbf{S}_1 \cdot \mathbf{I}_1 + A_2\mathbf{S}_2 \cdot \mathbf{I}_2, \quad (7)$$

but this approach essentially applies also to axially symmetric interactions. The resulting first order energy contributions on the diagonal of the Hamiltonian matrix are to be compared with those resulting from the term

$$\mathcal{H}' = A'_1\mathbf{S}' \cdot \mathbf{I}_1 + A'_2\mathbf{S}' \cdot \mathbf{I}_2 \quad (8)$$

in the empirical spin Hamiltonian in Part I. For the $S' = 1/2$ state this results in the equation $3(A'_1m_{I_1} + A'_2m_{I_2}) = 5A_1m_{I_1} - 2A_2m_{I_2}$ which gives $A_1 = (3/5)A'_1$ and $A_2 = -(3/2)A'_2$. The relations for all three spin states are included in Table 1. In this way the actual hyperfine parameters A_1 and A_2 which will be used for further analysis are expressed in the experimental values A'_1 and A'_2 .

3. Atomic Wave Function Parameters for Au and Fe

For gold the 5d, 6s, and 6p atomic orbitals need consideration. The electronic structure of the free gold atom has a closed 5d shell: 5d¹⁰6s. In a solid or in molecules 5d electrons are apt to hybridize or are subject to promotion to the 6s and 6p states, so that holes in the 5d shell can result.

Table 2
Atomic wave function parameters for gold in several electronic configurations

configuration	$\langle r^{-3} \rangle_{5d}$ (\AA^{-3})		$ \psi_{6s}(0) ^2$ (\AA^{-3})	$\langle r^{-3} \rangle_{6p}$ (\AA^{-3})
	one-electron value	collective value		
5d ^{7*})	106.4	-53.2	—	—
5d ^{8*})	99.4	49.7	—	—
5d ⁹ 6s ^{2*})	90.0	90.0	—	—
5d ^{9*})	92.5	92.5	—	—
5d ^{10*})	85.0	0	—	—
5d ¹⁰ 6s ^{**})	96.5	0	260	—
5d ¹⁰ 6s ^{***})	—	—	276	—
5d ¹⁰ 6p ^{****})	—	—	—	41

*) Hartree-Fock calculation, [15].

**) Hartree-Fock calculation, [13, 14].

***) Atomic beam experiment, [17].

****) Resonance scattering experiment, [19].

From approximate Hartree-Fock calculations by Herman and Skillman [13] (see [14]) and from similar calculations by Fraga et al. [15], values of $\langle r^{-3} \rangle_{5d}$ for various configurations can be derived, as given in Table 2. For a lower occupation of the 5d shell, higher values are found. This brings us to an estimate of 90 \AA^{-3} for a nearly completely filled 5d shell. All values are one electron values. Actually the unpaired electron spin can originate from a number of missing d-electrons. Due to Hund's rule, their spins are parallel and add up algebraically, so that one should consider the total charge distributions of the various configurations and their resulting $\langle r^{-3} \rangle$ values. For a closed 5d shell the contributions of the various electrons give rise to an effective value $\langle r^{-3} \rangle^{\text{eff}} = 0$, as a matter of fact. These effective values are also given in Table 2. For a transition metal ion in a crystal field of tetrahedral $\bar{4}3m(T_d)$ symmetry, these values do not apply, as there is a splitting of the d-levels. The three triplet states d_{xy} , d_{yz} , and d_{zx} add up to an electron distribution which produces an isotropic hyperfine interaction, forming a kind of closed subshell, as well as the doublet states $d_{x^2-y^2}$ and d_{z^2} . This means that the only possible deviation from an isotropic interaction results from only one missing or excess d-electron. For lower symmetry the triplet and/or doublet split even further, so that the same is still true. An illustration is given in Fig. 1.

Extrapolation of data from Herman and Skillman for the 6s orbital [14] and use of an empirical relativistic correction formula for heavy nuclei [16] leads to $|\psi_{6s}(0)|^2 = 260 \text{ \AA}^{-3}$. Also experimental data are available. In an atomic beam experiment, Wessel and Lew [17] determined the hyperfine interaction of atomic Au in the $^2S_{1/2}$ ground state, resulting in $|\psi_{6s}(0)|^2 = 276 \text{ \AA}^{-3}$. Similar agreement follows from the experimental value of 256 \AA^{-3} from an EPR experiment on Au^0 in NaCl, in which ionic matrix the atomic 6s electron is believed to be still localized on the gold atom [18].

No theoretical estimate for the 6p orbital is available. Experimental data exist however. The excited 6p $^2P_{3/2}$ state of gold has been investigated by resonance light scattering [19]. From the observed quadrupole effect, using the known electric quadrupole moment of ^{197}Au , a value $\langle r^{-3} \rangle_{6p} = 41 \text{ \AA}^{-3}$ can be evaluated. No Sternheimer nuclear shielding or antishielding factor is incorporated, although it may change the value by up to $\pm 30\%$ for heavy nuclei (e.g. [20]). The experimental accuracy of the above value is not very large either.

As ^{57}Fe is a widely used nucleus in Mössbauer spectroscopy, numerous calculations on various electronic configurations of iron ions are available. In most compounds

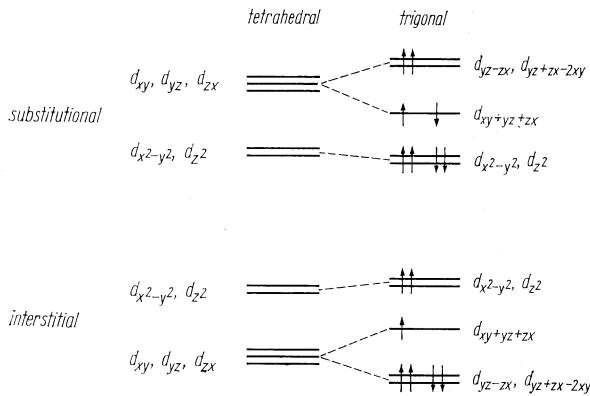


Fig. 1. Electronic d-states of a substitutional and an interstitial transition metal ion in a tetrahedral and trigonal crystal field. Occupation of the levels for Au^{2+} and Fe^{3+} are indicated

Table 3

Atomic wave function parameters for iron in several electronic configurations (one-electron values)

configuration	$\langle r^{-3} \rangle_{3d} (\text{\AA}^{-3})$		
	$3d^n$	$3d^n 4s 4p$	
n	**)	**)	***)
3	—	—	45.4
4	—	—	41.3
5	44.0	42.6	37.3
6	39.7	38.6	33.5
7*)	35.5	34.4	30.0
8*)	31.2	30.1	26.5
9*)	26.9	25.8	23.5
	$\langle r^{-3} \rangle_{3d} (\text{\AA}^{-3})$		$ \psi_{4s}(0) ^2 (\text{\AA}^{-3})$
$3d^6 4s^2$ *****)	38.2		32.6
*****)	—		25.1

*) Extrapolations.

**) Relativistic self-consistent field calculations, [21].

***) Hartree-Fock calculations, [22].

*****) Hartree-Fock calculations, [13, 14].

*****) Hartree-Fock calculations, [23, 24].

iron ions are positive with one or two electrons in 4s orbitals. Interstitial transition metal impurities in silicon, on the other hand, confine their electrons to the 3d shell and may adopt negative charge states. Consequently their 3d shells will have a higher occupation, so that we had to extrapolate available calculated results to $3d^7$, $3d^8$, and $3d^9$ configurations. Relativistic self-consistent field [21] and Hartree-Fock [22] calculations give a comparable dependence of $\langle r^{-3} \rangle_{3d}$ on the 3d configuration. These results and our extrapolations are also given in Table 3.

Hartree-Fock results by Herman and Skillman [13] (see [14]) and Watson et al. [23, 24] for the 4s orbital are also included in Table 3. Calculations on the 4p orbital have not been found.

4. Analysis and Discussion

In the preceding sections we indicated that an LCAO description presents the easiest way to analyse hyperfine interactions. Arguments against such a simple picture have already been mentioned. Nevertheless we will shortly consider it, before going to an analysis which makes allowance for the many electron character of the system. The justification for an LCAO description is generally found in the fact that a lattice imperfection can be described with a single unpaired electron which is shared over some atom sites. In order to arrive at this situation, an important requirement must be met: both the Fe-3d and Au-5d shells have to be filled completely. Such a configuration can only be achieved if the gold atom does not occupy a regular substitutional site.

A first possibility is that, just like iron, also gold is interstitial. This is considered rather improbable in Part I of this article. Another possibility is the vacancy-inter-

Table 4
Analysis of hyperfine data according to different possible models (see text)

LCAO model	$\text{Au}_s^0\text{Fe}_i^0$				$\text{Au}_s^-\text{Fe}_i^+$											
	a (MHz)	b (MHz)	$\frac{\text{s-p}}{\gamma^2}$	$\frac{\text{s-d}}{\gamma^2}$	a (MHz)	b (MHz)	$\frac{\langle r^{-3} \rangle_{\text{d}}^{\text{eff}}}{\langle r^{-3} \rangle_{\text{d}}^{\text{free}}}$	$\frac{ \psi(0) _{\text{d}}^2}{(\text{\AA}^{-3})}$	a (MHz)	b (MHz)	$\frac{\langle r^{-3} \rangle_{\text{d}}^{\text{eff}}}{\langle r^{-3} \rangle_{\text{d}}^{\text{free}}}$	$\frac{ \psi(0) _{\text{d}}^2}{(\text{\AA}^{-3})}$				
Au	33.4	6.0	0.27	0.04	0.96	0.175	0.06	0.94	20.0	3.6	0.10	1.7	50.0	9.0	0.24	4.2
Fe	14.6	-2.3	<0.20*		0.13	0.15	0.85	-21.9	3.5	3.5	0.17	1.0	8.8	-1.4	0.07	0.4
Si(3)	≤ 17	-	≤ 0.016	0.25	0.75											

*) Estimate from comparison with other nuclei.

stitial model by van Vechten and Thurmond [9]. In that case the electron bonds on the four silicon atoms around the gold site have to be reconstructed as if they surrounded a single lattice vacancy. Then the gold atom needs no longer to supply electrons for covalent bonds. When we apply this model to the Au-Fe complex, it is hard to imagine how to conserve trigonal symmetry. In such a Au_iFe_i complex, either with or without a vacancy, we arrive at a $\text{Au}^+-5\text{d}^{10}\text{-Fe}^{2+}\text{-}3\text{d}^{10}$ configuration where the paramagnetism arises from a bound hole. This model is reminiscent of the model which has been proposed for substitutional Pd and Pt in silicon [6]. Only in this model an LCAO analysis deserves further discussion.

By substitution of the experimental data for the hyperfine parameters a and b as presented in Part I and the wave function parameters of Section 3 into (2) and (3), we can derive the distribution of the electron over the atomic orbitals. The resulting values for the localization are given in the first part of Table 4. The anisotropic parts of the hyperfine interactions may arise from d- as well as from p-orbitals. Both possibilities are considered.

For the gold orbitals a lower limit for the quadrupole interaction is available. Using (6), the experimental limit of $P = 15$ MHz just corresponds with the value $\eta_{\text{Au}}^2\gamma_{\text{Au}}^2 = 0.165$ for a 5d orbital. Agreement is also obtained for a 6p orbital as an even larger value of P results in that case.

On the two transition atoms a total localization of 30% is found when taking d-orbitals and about 45% taking p-orbitals. The anisotropy of the hyperfine interactions with three ^{29}Si neighbour sites could not be resolved due to overlap with the central EPR lines. It is customary to assume sp^3 hybrids on these sites. Using wave function parameters from [10], this accounts for 5% of the electron wave function. Localization on further silicon lattice sites gives rise to unresolved hyperfine interactions, constituting the inhomogeneous EPR linewidth. The linewidth reported in Part I is comparable to those observed for lattice defects. Electron nuclear double resonance data of the divacancy indicate that such smaller interactions can account for another 30% of the electron [25, 26].

In addition to earlier objections against a Au_iFe_i structure, the above results leave some questions. Firstly a bound hole wave function can only be formed from a combination of occupied orbitals, so that the unoccupied Au-6s and Fe-4s orbitals cannot contribute. As the 5s/3s orbitals are too distant in energy, the origin of the isotropic interaction is not clear if it is from a bound hole. The same argument only leaves d-orbitals for the isotropic interaction. In the second place the total localization is remarkably small. Especially when choosing d-orbitals in the LCAO wave function 35% is left unexplained. Finally there is no explanation for the opposite signs of a_{Fe} and b_{Fe} .

A more promising approach is a description of two coupled electron spins as introduced in Section 2.2. Strong antiferromagnetic coupling gives an effective total spin $S' = 1/2$, as observed experimentally. This spin can arise from either a $\text{Au}_s^0\text{Fe}_i^0$ or a $\text{Au}_s^-\text{Fe}_i^+$ complex. Both possibilities will be considered here. In the model of coupled spins we can still adopt (2), (3), and (6), if we replace the quantities $\eta^2\alpha^2|\psi_s(0)|^2$, $\eta^2\beta^2\langle r^{-3}\rangle_p$, and $\eta^2\gamma^2\langle r^{-3}\rangle_d$ by effective wave function parameters $|\psi_s(0)|_{\text{eff}}^2$ and $\langle r^{-3}\rangle_{p/d}^{\text{eff}}$.

In order to know which d-shell configurations follow for different charge states of the two impurity atoms, a schematic energy level diagram is given in Fig. 1. It shows the splitting of the triplet state if the symmetry is lowered from tetrahedral to trigonal. The shapes of the d-orbitals as derived from group theory are also indicated, expressed in the usual way in x , y , and z coordinates. The singlet orbital $d_{xy+yz+zx}$ has the trigonal $\langle 111 \rangle$ direction as its symmetry axis.

First we will pay attention to the anisotropic part of the hyperfine interaction, i.e.

to the d-orbitals. In $\text{Au}_s^0\text{Fe}_i^0$ the Ludwig-Woodbury model gives a configuration $\text{Au-5d}^7\text{6s6p}^3\text{-Fe-3d}^8$, with respectively spins of $S_1 = 3/2$ and $S_2 = 1$, due to three and two missing d-electrons. If we derive the actual hyperfine interaction in the way described in Section 2.2, we obtain the values given in Table 4. The resulting values $\langle r^{-3} \rangle_{3d}^{\text{eff}} = 4.5 \text{ \AA}^{-3}$ and $\langle r^{-3} \rangle_{5d}^{\text{eff}} = 8.7 \text{ \AA}^{-3}$ are clearly much smaller than the one-electron values in Tables 2 and 3.

On the other hand, Fig. 1 shows that the $\text{Au}_s\text{-5d}^7$ and $\text{Fe}_i\text{-3d}^8$ configurations both form filled sub-shells as mentioned in Section 3, leading theoretically to $\langle r^{-3} \rangle^{\text{eff}} = 0$. In that case we should account for the observed values by a fractional charge transfer. On the gold atom 10% of an electron from the bond orbitals might occupy the singlet level. On the iron atom 17% of the electron in the singlet level might be promoted to a 4s orbital, leaving a fraction of a hole in the closed sub-shell. In both cases the right axial symmetry direction follows.

A discrepancy enters when we consider the quadrupole interaction with the gold nucleus. The resulting value $\langle r^{-3} \rangle_{5d}^{\text{eff}} \geq 16 \text{ \AA}^{-3}$ cannot be brought into agreement with the value of 9 \AA^{-3} , obtained from the hyperfine interaction. This brings us to the alternative model of a $\text{Au}_s^-\text{Fe}_i^+$ complex, which for other reasons is considered more probable in Part I. The configuration $\text{Au}^-\text{5d}^8\text{-Fe}^+\text{-3d}^7$ gives rise to spins $S_1 = 1$ and $S_2 = 3/2$, which leads to a total spin $S' = 1/2$. In this case the subscripts in Table 1 have to be interchanged. We then arrive at different actual hyperfine parameters giving $\langle r^{-3} \rangle_{3d}^{\text{eff}} = 1.8 \text{ \AA}^{-3}$ and $\langle r^{-3} \rangle_{5d}^{\text{eff}} = 21 \text{ \AA}^{-3}$. In this way the hyperfine interaction is brought into agreement with the result of the quadrupole interaction.

On the other hand, we have arrived at a case where on the gold atom the singlet level $d_{xy+yz+zx}$ is occupied above a closed sub-shell, while on the iron atom the electron of the singlet level is missing from a closed sub-shell. The obtained $\langle r^{-3} \rangle_d^{\text{eff}}$ values are much smaller than the free atom values for entire d-orbitals. In particular for iron there is a factor of 14 difference.

At this stage it is worthwhile to consider the abundant amount of data on single transition impurities and impurity pairs in silicon [3] and on iron-defect complexes [27]. These hyperfine data can easily be corrected for differences in the nuclear magnetic moments which enter in (2) and (3). Then in all cases values of the same order of magnitude follow, irrespective of the d-shell configuration. This indicates that there is a more general reason why the $\langle r^{-3} \rangle_d^{\text{eff}}$ values for transition metals in silicon are much smaller than for free atoms. Reduction of $\langle r^{-3} \rangle_d$ values which has been observed in other materials to a much lesser extent, is often accounted for by hybridization or by admixture of nearest neighbour ligand orbitals. From the observed small localization on nearby lattice sites, it follows that in this case such effects do not contribute appreciably. In a review on iron group ions in tetrahedral coordination by Ham and Ludwig [28], this has already been recognized. As another phenomenon which affects the transition metal wave functions, they mention covalency of the host lattice. In a covalent solid like silicon this will clearly be a main effect. However, the case of silicon has explicitly been left out of consideration by Ham and Ludwig.

The isotropic part of the hyperfine interaction is the other parameter to account for. The effective values $|\psi(0)|_{\text{eff}}^2$ which follow in the two alternative cases are included in Table 4. In a model where the electron spin primarily arises from d-electrons, it is difficult to explain the isotropic hyperfine interaction from occupation of the outer s-orbitals. From experiments in many other materials, as well as from theoretical calculations [23], it is known that transition ions show a pronounced core polarization. This polarization of the closed inner s-shells is due to the unpaired spins in the outer d-shell. The net unpaired spin of the successive s-shells tends to be of opposite sign. For iron this results in a net spin which is opposite to the 3d electron spins. This readily

explains the opposite signs of a_{Fe} and b_{Fe} . Both theoretically and experimentally in most substances the unpaired spin due to core polarization in iron can be determined to be equivalent to an unpaired spin density $|\psi(0)|^2 \approx 7 \text{ \AA}^{-3}$ for a $3d^6$ configuration [23]. For configurations with a different number of unpaired 3d electrons this value should proportionally be changed. For 5d transition metals like gold, calculations yielded even larger core polarizations, equivalent to a value of $|\psi(0)|^2 \approx 10 \text{ \AA}^{-3}$ per unpaired 5d electron [29]. The experimental values in silicon tend to be nearly an order of magnitude smaller, not only for the present EPR spectrum, but as well for all the other reported spectra [3, 27].

5. Conclusions

From the preceding analysis and discussion we conclude that the EPR spectrum which is described in Part I arises from two exchange coupled electron spins. A substitutional negative gold ion gives an electron spin $S = 1$. An interstitial positive iron ion has electron spin $S = 3/2$. Strong antiferromagnetic coupling leads to a total effective spin $S' = 1/2$.

The wave function parameters $\langle r^{-3} \rangle_d$ which can be derived from the hyperfine interaction are about an order of magnitude smaller than the values for a free atom. The isotropic hyperfine interaction is thought to arise from core polarization. Also this effect is an order of magnitude smaller than in most other materials. An explanation for the smaller $\langle r^{-3} \rangle_d$ values has to be found in the covalency of silicon. Due to a kind of screening, the d-orbitals may appreciably be expanded with respect to the free atom orbitals. This delocalization of the d-orbitals may also reduce the core polarization.

For a quantitative confirmation of these suppositions, we have to wait for application of modern theoretical computation techniques to these problems. Calculations based upon LCAO principles, although useful for lighter nuclei like carbon and even silicon, do not lead to satisfactory results for heavier nuclei and certainly not for transition metal atoms. Very recently spin restricted scattered-wave X α calculations on interstitial transition metal ions in silicon have been performed by DeLeo et al. [30]. Their results point into the same direction as our experimental observations. The Green's function approach which has recently been applied to lattice defects in silicon, may also give interesting results for transition metal impurities.

References

- [1] G. W. LUDWIG and H. H. WOODBURY, Phys. Rev. Letters **5**, 98 (1960).
- [2] H. H. WOODBURY and G. W. LUDWIG, Phys. Rev. **117**, 102 (1960).
- [3] G. W. LUDWIG and H. H. WOODBURY, Solid State Phys. **13**, 223 (1962).
- [4] H. FEICHTINGER, in: Defects and Radiation Effects in Semiconductors 1978, Ed. J. H. ALBANY, Institute of Physics, London 1979 (p. 528).
- [5] G. W. LUDWIG and H. H. WOODBURY, Phys. Rev. **117**, 1286 (1960).
- [6] H. H. WOODBURY and G. W. LUDWIG, Phys. Rev. **126**, 466 (1962).
- [7] H. H. WOODBURY and G. W. LUDWIG, Phys. Rev. **117**, 1287 (1960).
- [8] H. G. GRIMMEIS, Annu. Rev. Mater. Sci. **7**, 341 (1977).
- [9] J. A. VAN VECHTEN and C. D. THURMOND, Phys. Rev. B **14**, 3539 (1976).
- [10] G. D. WATKINS and J. W. CORBETT, Phys. Rev. **134**, A1359 (1964).
- [11] T. P. DAS and E. L. HAHN, Solid State Phys., Suppl. **1**, 1 (1958).
- [12] C. H. TOWNES and B. P. DAILEY, J. chem. Phys. **17**, 782 (1949).
- [13] F. HERMAN and S. SKILLMAN, Atomic Structure Calculations, Prentice Hall, Inc., Englewood Cliffs (N.J.) 1963.
- [14] J. R. MORTON and K. F. PRESTON, J. magnetic Res. **30**, 577 (1978).

- [15] S. FRAGA, K. M. SAXENA, and J. KARWOWSKI, Handbook of Atomic Data, North-Holland Publ. Co., Amsterdam 1976.
- [16] J. H. MACKAY and D. E. WOOD, J. chem. Phys. **52**, 4914 (1970).
- [17] G. WESSEL and H. LEW, Phys. Rev. **92**, 641 (1953).
- [18] P. G. BARANOV, R. A. ZHITNIKOV, and V. A. KHRAMTSOV, phys. stat. sol. (b) **76**, K109 (1976).
- [19] G. GOLDMANN, C. HAHN, and J. NEY, Z. Phys. **225**, 1 (1969).
- [20] A. ROSÈN, Physica Scripta **8**, 159 (1973).
- [21] J. L. K. F. DE VRIES, J. M. TROOSTER, and P. ROS, J. chem. Phys. **63**, 5256 (1975).
- [22] S. K. LIE, D. M. S. ESQUIVEL, and D. GUENSBURGER, Chem. Phys. Letters **57**, 458 (1978).
- [23] R. E. WATSON and A. J. FREEMAN, Phys. Rev. **123**, 2027 (1961).
- [24] R. E. WATSON and L. H. BENNETT, Phys. Rev. B **15**, 502 (1977).
- [25] J. G. DE WIT, C. A. J. AMMERLAAN, and E. G. SIEVERTS, in: Lattice Defects in Semiconductors 1974, Ed. F. A. HUNTLEY, Institute of Physics, London 1975 (p. 178).
- [26] E. G. SIEVERTS, S. H. MULLER, and C. A. J. AMMERLAAN, Phys. Rev. B **18**, 6834 (1978).
- [27] S. H. MULLER, G. M. TUYNMAN, E. G. SIEVERTS, and C. A. J. AMMERLAAN, Phys. Rev. B, to be published.
- [28] F. S. HAM and G. W. LUDWIG, in: Paramagnetic Resonance, Vol. 1, Ed. W. Low, Academic Press Inc., New York 1963 (p. 130).
- [29] A. J. FREEMAN, J. V. MALLOW, and P. S. BAGUS, J. appl. Phys. **41**, 1321 (1970).
J. P. DESCLAUX, A. J. FREEMAN, and J. V. MALLOW, J. Magnetism magnetic Mater. **5**, 265 (1977).
- [30] G. G. DELEO, G. D. WATKINS, and W. B. FOWLER, Phys. Rev. B **23**, 1851 (1981).

(Received August 26, 1981)